HHS Public Access

Author manuscript

*Integr Biol (Camb)*. Author manuscript; available in PMC 2018 March 14.

Published in final edited form as:

*Integr Biol (Camb)*. 2014 March ; 6(3): 348–356. doi:10.1039/c3ib40225h.

# Ligand density elicits a phenotypic switch in human neutrophils

**Steven J. Henry**[a], **John C. Crocker**[b], and **Daniel A. Hammer**[a,b]

[a]Department of Bioengineering, University of Pennsylvania, 210 S 33rd St, Philadelphia, PA 19104

[b]Department of Chemical and Biomolecular Engineering, University of Pennsylvania, 220 S 33rd St, Philadelphia, PA 19104

## Abstract

Neutrophils are mediators of innate immunity and motility is critical to their function. We used microcontact printing to investigate the relationship between density of adhesive ligands and the dynamics of neutrophil motility. We show that neutrophils adopt a well-spread morphology without a uropod on moderate densities of adhesion ligand. As density is increased, the morphology switches to a classic amoeboid shape. In addition to the morphological differences, the dynamics of motility were quantitatively distinct. Well-spread cells without uropods glide slowly with high persistence while amoeboid cells made frequent directional changes, migrating quickly with low persistence. Using an antibody panel against various integrin chains, we show that adhesion and motility on fibronectin were mediated by MAC-1 ($\alpha_M\beta_2$). The phenotypic switch could be generalized to other surface ligands, such as bovine serum albumin, to which the promiscuous MAC-1 also binds. These results suggest that neutrophils are capable of displaying multiple modes of motility as dictated by their adhesive environment.

## Introduction

Leukocytes are important mediators of immunity, and motility is critical to their function. Neutrophils in particular act as first responders to pathogen challenges[1] as well as sterile trauma[2] resulting in inflammation. The role of soluble chemoattractants in stimulating and directing neutrophil motility has long been of interest[1] and has been explored in various engineered *in vitro* systems[3]. Recently, attention has shifted to environment dimensionality in dictating the mode of leukocyte migration[4]. As the empirical body of leukocyte observations has grown, it is now appreciated that these cells can employ an assortment of migratory mechanisms.

On a majority of two-dimensional *in vitro* substrates, neutrophils exhibit an amoeboid morphology.[3, 5] The distinguishing features of this phenotype are an elongated cell body with a frontward ruffled-lamellipodium, a midregion that contains the nucleus, and rearward knob-like uropod.[5a] Detailed images of this morphology have been captured with high

hammer@seas.upenn.edu.

†Electronic Supplementary Information (ESI) available: Movie S1, Movie S2, and a PDF containing Supplementary Fig.1-7 and associated text. See DOI: 10.1039/b000000x/

resolution scanning electron microscopy (SEM).[6] However, there have also been observations of neutrophils assuming a very different, well-spread phenotype without uropods on two-dimensional substrates.[7] In those instances the alternative phenotype was attributed to the underlying stiffness of the material, as neutrophils on softer substrates were shown to reassume an amoeboid phenotype. Yet, neutrophils also display the amoeboid phenotype on stiff substrates, such as those in the previously cited SEM studies, suggesting substrate stiffness is not a unique controller of cell morphology.[8] Hypothesizing that another factor was involved in modulating these two phenotypes, our study focused on the role of ligand density.

In this paper, we investigated neutrophil morphology and motility on increasing densities of the extracellular matrix protein fibronectin (FN). We observed that neutrophils exhibited a well-spread, uropod-absent phenotype on sub-saturating, intermediate densities of FN. On high densities of ligand this phenotype was replaced with the amoeboid phenotype. The modes of motility associated with these two morphologies were quantifiably distinct as shown by comparison of their mean squared displacement with time. Finally, we determined that the FN adhesion and motility were mediated by MAC-1 ($\alpha_M\beta_2$). The phenotypic switch could be generalized to other surface ligands, such as bovine serum albumin, to which the promiscuous MAC-1 also binds.

## Materials and Methods

### Media

Rinsing buffer was Hanks' Balanced Salt Solution (Invitrogen, Carlsbad, CA) without calcium or magnesium supplemented with 10 mM HEPES (Invitrogen) and pH adjusted to 7.4. Storage buffer was rinsing buffer supplemented with 2 mg/mL glucose. Running buffer was storage buffer supplemented with 1.5 mM $Ca^{2+}$ and 2 mM $Mg^{2+}$. Fibronectin (FN) was from human plasma (BD Biosciences, Bedford, MA). Low-endotoxin bovine serum albumin (BSA) (Sigma) was prepared at 2% and 0.2% w/v in PBS without calcium and magnesium (PBS(−)). Labeling of proteins via Alexa Fluor carboxylic acid, succinimidyl ester (Invitrogen) was performed in accordance with the manufacturer's recommended protocol. Stock N-formylmethionyl-leucyl-phenylalanine (fMLF) (Sigma, Saint Louis, MO) was reconstituted in glacial acetic acid before dilution. The nonionic triblock copolymer Pluronic F-127 (Sigma) was prepared at 0.2% w/v in PBS(−). All solutions were sterile filtered or prepared sterile. Bicinchoninic acid protein assays (Pierce Biotechnology, Rockford, Il) were performed on stock solutions of proteins to measure concentration.

### Substrates

Poly(dimethylsiloxane) (PDMS) (Sylgard 184 Silicone Elastomer, Dow Corning, Midland, MI) coated coverslips were prepared from number one thickness glass coverslips (Fisher Scientific, Hampton, NH) of 25 mm diameter spun with degassed PDMS (10:1 base:cure by weight). Spinning at 4000 rpm for 1 min, leveling at RT, and baking at 65 °C overnight resulted in a 12.5 ± 0.4 μm layer of PDMS. Bare glass coverslips were cleaned via piranha wash (2:1 by volume $H_2SO_4$:$H_2O_2$) and thoroughly rinsed in di$H_2O$. Coverslips were dried completely in a 90°C oven. Coverslips, bare and PDMS-coated, were affixed to the bottom

of six-well tissue culture plates which had either been hot-punched or laser-cut to generate a 22 mm diameter opening in the bottom of the wells. Coverslip bonding was performed using a continuous bead of Norland Optical Adhesive 68 (Thorlabs, Newton, NJ), cured for 20 min under a long wavelength ultraviolet lamp.

## Protein Deposition and Blocking

Stamps for printing were prepared from PDMS, mixed at 10:1 base:cure by weight, degassed, and poured over a silicon wafer. The polymer was cured by baking for 2 hr or longer at 90°C. Trimmed stamps were sonicated in 200 proof ethanol for 10 min, rinsed twice in di$H_2O$ and dried in a gentle stream of filtered $N_{2(g)}$. The face of the PDMS stamp previously cast against the silicon wafer was covered with a sessile drop of protein solution. After incubation, stamps were rinsed twice in a submerging quantity (~ 50 mL) of di$H_2O$ and dried in a gentle stream of filtered $N_{2(g)}$. For motility studies stamps were 1 $cm^2$, inked with 200 μL of protein solution for 2 hrs at RT. For all other experiments, stamps were 0.36 $cm^2$, inked with 50 μL of protein solution for 1 hr at RT. After stamp inking and drying, mounted PDMS-coated coverslips were treated for 7 min with ultraviolet ozone (UVO Cleaner Model 342, Jelight, Irvine, CA) to render the surface hydrophilic.[9] Stamps were placed in conformal contact with the activated substrate for approximately 30 s.

For physisorption experiments, sterile flexiPERM (Sigma) silicone gaskets were affixed to the substrates to hold an aliquot of protein at a concentration and volume that preserved the number of protein molecules per unit area of exposed surface for comparison with the printed conditions.

Blocking printed or adsorbed surfaces by submersion in 0.2% w/v solutions of Pluronic F-127 or BSA (0.2% or 2%) was performed for 1 hr. Native glass is not amenable to Pluronic blocking until silanized by immersion in 5% dimethyl dichlorosilane (Sigma) in dicholorobenzene (Sigma).[10] After blocking, each well was rinsed four or five times with 2 mL PBS(−) without dewetting the functionalized surface to prevent Pluronic sloughing. If substrates were not used the day of fabrication, they were stored overnight at 4 °C under PBS(−). Prior to cell plating, storage PBS(−) was exchanged for running buffer, without dewetting, and equilibrated to 37°C at 5% $CO_2$ in a cabinet incubator.

## Neutrophil Isolation

Whole blood was obtained from human donors via venipuncture and collection in heparin vials. Samples were collected with University of Pennsylvania Institutional Review Board approval from consenting adult volunteers. Volunteers were required to be in good health and abstain from alcohol and all over-the-counter medication for 24-48 hrs prior to donation. Blood samples were allowed to cool to RT (15-30 min) and layered in a 1:1 ratio of whole blood to Polymorphprep (Axis-Shield, Oslo, Norway). Vials were spun for 45 min at 500×g and 21°C. After separation, the polymorphonuclear band and underlying separation media layer were aspirated into fresh round-bottom tubes. The isolated solution of cells and separation-media was diluted with rinsing buffer and spun for 5 min at 350×g and 21°C. Red Blood Cells (RBC) were eliminated from the resulting cell pellet via hypotonic lysis. After lysis, vials were centrifuged for 5 min at 350×g and 21°C and the RBC-free pellets

resuspended in storage buffer. Neutrophils were stored at $5 \times 10^5$ - $1 \times 10^6$ cells/mL on a tube rotisserie at 4°C until time of plating.

## Cell Motility Experiments

For a given experimental condition, $7.5 \times 10^4$ neutrophils were seeded on a pre-equilibrated substrate under 1.5 mL of running buffer. Visual confirmation was made that cells had a rounded (i.e. not polarized) morphology at time of plating. Substrates and cells were incubated 10 min at 37°C and 5% $CO_2$ to allow settling and gently rinsed twice with 1 mL of fresh running buffer to remove non-adherent cells. Prior to rinsing, visual observation of the cells confirmed a transition from rounded to a well-spread. Cell density was minimized to prevent cell-cell collisions but sufficiently dense to acquire reasonable sample sizes for statistical testing. Adherent neutrophils at multiple locations on the same substrate were imaged by time-lapse videomicroscopy for 30 min or longer at 30-90 s intervals in a temperature controlled chamber.

Phase-contrast image stacks corresponding to each imaging location of a particular experimental condition were processed via a custom MATLAB (The MathWorks, Natick, MA) script that identified cell boundaries, computed geometric centroids, and connected centroids in consecutive frames to form trajectories. Portions of trajectories were only retained for cells prior to cell-cell collisions and for cells that did not undergo apoptosis. To improve statistical power, multiple locations were imaged per condition. Summing across all field of views (FOVs) acquired we observed a total of 2688 neutrophils, 60% of which (n = 1606) where tracked and their trajectories utilized in MSD construction and curve fitting. Within this group of observed and tracked cells 75% (n = 1204) were tracked for the entire duration of the 30 min observation window and used in model-independent analyses. The remaining cells were tracked for only a portion of that observation window as they subsequently underwent cell-cell collisions. Of those cells that were observed but not tracked (n = 1082), 88% were excluded on the basis of cell-cell contact, residing at the edge of the FOV, or exiting the FOV. The remaining 12% were excluded on the basis of having an anomalous phenotype (e.g. appearing apoptotic). Cell tracking, mean-squared displacement computation, and error analysis were based upon the multiple particle tracking method reviewed by Crocker and Hoffman[11].

## Integrin Blocking

The following panel of function-blocking antibodies against various integrin chains was assembled and used at final concentrations of 50 μg/mL: anti-$\beta_1$ clone MAb13 (BD Biosciences), anti-$\beta_2$ clone L130 (BD Biosciences), anti-$\alpha_M$ clone ICRF44 (eBioscience), and anti-$\alpha_5$ clone SAM1 (eBioscience). Isotype controls to IgG1 and IgG2a were purchased from eBioscience. $5 \times 10^5$ neutrophils in 200 μL running buffer were incubated for 10 min with antibodies at RT with periodic mixing before exposure to the FN substrate. Substrates and cells were incubated 10 min at 37°C and 5% $CO_2$ and immediately fixed in a solution of 4% formaldehyde (Fisher) or 10% neutral buffered formalin (Sigma) for 30 min at RT with periodic mixing. After fixation substrates were rinsed thoroughly with PBS to remove nonadherent cells.

## Results and Discussion

### Observation of Neutrophil Phenotypes on Two Different Substrates

A common method of preparing two-dimensional surfaces for motility studies is to adsorb an adhesive ligand onto glass or polystyrene and subsequently wash with a solution of bovine serum albumin (BSA). The BSA wash is intended to mask bare regions of the substrate, unoccupied by protein, and impede non-specific cell-substrate interactions. When we plated human neutrophils on such a surface (fibronectin (FN)-adsorbed and BSA-blocked) the cells assumed an amoeboid phenotype having elongated cell bodies, trailing uropods, and narrow lamellipodia (Fig. 1a). The associated motility was undular, with cells undergoing frequent directional changes (Movie S1). The amoeboid phenotype has been reported elsewhere[3, 5-6] for neutrophils on various two-dimensional surfaces. By contrast, when we printed a poly(dimethylsiloxane) (PDMS) surface with FN and blocked with Pluronic, we elicited a very different phenotype. In the latter case the neutrophils were highly spread and no trailing uropods were discernible (Fig. 1b). With this phenotype, the cells appeared to glide and were highly persistent in their direction (Movie S2). Our impression is that this latter phenotype was more qualitatively reminiscent of fish-keratocytes[8a] than amoeboid cells.

Complementary controls of neutrophils on FN-printed glass FN-adsorbed PDMS demonstrated that the phenotypic differences depended on the blocking agent, not the method of protein deposition (Supplementary Fig. 1a-d). Quantitative fluorescence measurements of fluorophore-labeled FN confirmed that total FN loading of glass and PDMS surfaces were comparable (Supplementary Fig. 1e). When we silanized glass and then blocked surfaces with Pluronic, we found the well-spread, uropod-absent phenotype could be elicited on FN functionalized glass (Supplementary Fig. 2a). Our interpretation is that when blocking with Pluronic, cell binding was solely due to the underlying FN, and the blocking agent did not contribute to the adhesion (Supplementary Fig. 3c-e).

We hypothesized that the amoeboid phenotype is a result of adhesion to high densities of surface ligand, and that blocking with BSA served to increase the total ligand content. To test this hypothesis, we used microcontact printing to systematically control the density and type of surface ligand (Supplementary Fig. 4a). Microcontact printing is a tool to spatially pattern cellular adhesive ligands[9, 12] and to print the tips of polymeric posts for force measurements[13]. While microcontact printing has been extensively used to study the behavior of mesenchymal[9, 12-14] cells, it has only recently been applied in studies of hematopoietic-derived cells[15]. In our study, microcontact printing was used to immobilize different densities of FN on PDMS. By titrating the inking concentration of the protein solution used to prepare the stamps, we could reproducibly achieve sub-saturating densities of deposited FN (Supplementary Fig. 4b). After fabricating a series of PDMS surfaces with systematically varied densities of FN, all blocked with Pluronic F127, we scored the resulting neutrophil phenotypes observed (Fig. 2a).

On surfaces printed with little or no FN and blocked with Pluronic, cells failed to polarize or spread and remained spherical, presenting as bright white circles under phase contrast imaging (Fig. 2i). On intermediate densities of printed-FN, blocked with Pluronic, the well-

spread, uropod-absent phenotype was observed (Fig. 2ii). Frequency of the keratocyte-like phenotype peaked at 40% surface saturation. As density of FN increased, the well-spread phenotype was observed less frequently. Once surface density reached 83% saturation the amoeboid phenotype was predominate (Fig. 2iv).

Others have observed this well-spread, uropod-absent phenotype in neutrophils on FN-conjugated polyacrylamide gels[7]. In those instances the morphology was attributed to the underlying stiffness of the material, as neutrophils on softer gels were more amoeboid. Indeed, our relatively thick PDMS layers (~ 12 μm) and the use of a 10:1 formulation (base:cure, w/w) means the substrates were quite stiff, with Young's moduli on the order of megapascals[16]. However, here we demonstrated that the well-spread phenotype on stiff surfaces is only inducible for sub-saturating densities of ligand. This observation contributes to the growing empirical body of evidence showing neutrophils and other leukocytes can adopt a variety of motile mechanisms to achieve translocation and helps reconcile the occurrence of both phenotypes elsewhere in the literature of neutrophil motility on stiff substrates.

Ziebert and Aranson have constructed a biophysical model of cell motility that demonstrates phenotypic transitions in the mode of migration as a function of underlying substrate stiffness and surface adhesivity.[8b] On stiff substrates their model predicts a transition from stick-slip to gliding motion as surface ligand density is increased. While we have not observed stick-slip motion at low adhesivity we have found an intermediate ligand density window in which neutrophils display a highly persistent gliding phenotype. It will be interesting to see if the incorporation of intracellular viscoelasticity into their future models can recapitulate our transition from gliding motion to amoeboid motion at saturating conditions of adhesive ligand. A transition from gliding to more erratic motion has also been reported of fish keratocytes on stiff substrates as surface adhesivity increases.[8a]

Our study of how neutrophil phenotype depends on adhesion draws an interesting qualitative comparison with recent work on the capacity of physical confinement to dictate migratory cell phenotype. Migratory cells in physically confined channels or on narrow one-dimensional tracks of ligand have been shown to lose characteristics of conventional two-dimensional migration.[4c] Hung and co-workers have also found that the mechanism of propulsion differs as a function of substrate dimensionality.[17] In the future, immunocytochemical staining and small molecule inhibitor studies of our amoeboid versus keratocyte-like morphologies may reveal similar discrepancies driven by ligand density.

## Quantifying Motility of Amoeboid and Keratocyte-Like Phenotypes

The dynamics of amoeboid and keratoctye-like motility were distinct, as revealed by comparing their mean squared displacements (MSD) as a function of time (Fig. 3). On log-log axes, the slopes of MSD vs. time for the two populations were different. Neutrophils undergoing amoeboid migration accumulated squared displacement diffusively (slope ~ 1) while neutrophils undergoing keratocyte-like migration accumulated squared displacement superdiffusively (slope > 1). Fitting the curves for MSD vs. time with the persistent random walk model of cell kinesis[18] ($\langle MSD(\tau)\rangle = 2S^2P[\tau - P(1-\exp(-\tau/P))]$) allowed us to quantify neutrophil motility in terms of the best-fit parameters speed (S) and persistence (P). Doing

so confirmed our qualitative assessment that amoeboid motility was faster and less persistent ($S_{amoeboid}$ = 6 μm/min, $P_{amoeboid}$ = 0.5 min) than keratocyte-like motility ($S_{keratocyte\text{-}like}$ = 3 μm/min, $P_{keratocyte\text{-}like}$ = 15 min). Comparing the cytoskeletal architecture of these two dramatically different phenotypes remains to be done. It will be interesting to learn how stress fibers are organized in the keratocyte-like cell, compared to the amoeboid cell.

To this point neutrophils were induced to adhere and be motile on FN substrates without prior or concurrent stimulation by soluble chemoattractant. Therefore, the resulting motility was haptokinetic, driven by FN stimulation at the cell-substrate interface. A control study quantifying selectin-expression[19] via flow cytometry confirmed neutrophils were not primed for integrin-based adhesion to FN surfaces by virtue of isolation or storage stresses (Supplementary Fig. 5).

## Effect of Chemoattractant on Keratocyte-Like Motility

We explored the capacity of the potent neutrophil chemoattractant formyl-Met-Leu-Phe (fMLF)[20] to modulate the motility of neutrophils undergoing keratocyte-like migration. On 44% saturated FN surfaces, the addition of 10 nM fMLF to haptokinetic neutrophils had the effect of increasing the total dispersion of the cell system (Fig. 4a-b). To quantify the extent of motility in a model-independent fashion we extracted the maximum displacements for cells tracked over 30 min. Cell trajectories shorter than 30 min were excluded in this analysis to avoid inadvertently biasing the data. The mean of the maximum displacements ($\langle \max(|\Delta r|) \rangle$) was computed for each combination of FN adhesiveness and fMLF concentration (Fig. 4c). Introducing fMLF, after onset of FN-induced haptokinesis, potentiated motility in a dosage-dependent manner at an intermediate ligand density of 44% saturation. However, at a higher surface saturation of 73%, fMLF was no longer capable of increasing the basal motility induced by FN stimulation. The number of independent observations for each condition and a comprehensive description of mean maximum displacement data are reported in Supplementary Fig. 6.

Computation of the MSD provides dynamic information on the dispersion of cells and allows the incorporation of cell trajectories shorter than the total experimental acquisition time. Time and ensemble-averaged MSDs for each independent observation were computed from all available cell trajectories through 30 min. The MSDs corresponding to Fig. 4a-b data are reported in Fig. 4d. In general, on log-log axes, the slope of the MSD curves are relatively constant and greater than unity. This denotes superdiffusive motility in which cells accumulate squared displacement faster than expected by pure diffusion. Considering the best-fit parameters speed and persistence, systematic variation in the dose of fMLF alters cell speed at intermediate density FN (Fig. 4e), but not the persistence time for any of the FN-fMLF conditions tested (Fig. 4f). All MSDs-vs.-time contributing to construction of Fig. 4d are compiled in Supplementary Fig. 7 along with complete results of multiple comparisons testing on mean speed data.

In both analyses the capacity of chemoattractant to augment haptokinetic motility in the keratocyte-like phenotype was found to be a function of the underlying adhesiveness. This emphasizes the importance of considering the role of substrate adhesiveness in controlling

the cell response to the milieu of soluble chemoattractants and cytokines known to orchestrate directional motility during inflammation.

## Identifying Integrin Chains Responsible for Adhesion

To identify the integrin chains responsible for neutrophil binding to FN, function-blocking antibodies with previously demonstrated efficacy in leukocytes were employed.[21] Functional blocking of $\beta_2$ integrins (Fig. 5d) resulted in a substantial decrease in cell adhesion on FN relative to the positive control without antibody present (Fig. 5a). Targeting the $\alpha_M$ integrin, which coordinates with $\beta_2$ integrin to form the MAC-1 heterodimer, was also found to disrupt cell binding on FN significantly (Fig. 5f). In neither case did blocking $\beta_1$ (Fig. 5c) nor $\alpha_5$ (Fig. 5e) integrin chains disrupt binding. These results led us to attribute the observed FN-induced adhesion and subsequent haptokinesis to the $\beta_2$ and $\alpha_M$ integrin subunits, or the MAC-1 receptor.

In neutrophils there is known cross talk between $\beta_1$ and $\beta_2$ integrins when ligating extracellular matrix proteins such as FN.[21a, 22] Our finding that neutrophils utilize MAC-1 ($\alpha_M\beta_2$) on FN is consistent with other empirical observations. In particular van den Berg and coworkers demonstrated that stimulation of $\beta_1$ integrins yields $\beta_2$-mediated adhesion in neutrophils on FN that can be mitigated by function-blocking antibodies against MAC-1.[21a] Our blocking study is a probe on the long time-limit (i.e. minute length scale) adhesion of neutrophils to FN. Lishko and co-workers demonstrated that a balance of MAC-1 and VLA-5 ($\alpha_5\beta_1$) is required for neutrophil translocation on FN attributing MAC-1 to adhesion and VLA-5 to migration.[22] Our work reveals that the adhesive contribution of MAC-1 is the dominant ligated integrin and may explain the reduced speed of the keratocyte-like phenotype.

MAC-1 also binds to members of the Ig superfamily[23], such as ICAM-1, which illustrates the promiscuity of this integrin. We hypothesized that the emergence of the amoeboid phenotype on BSA-blocked surfaces of intermediate density FN was due to simultaneous binding of MAC-1 to BSA and FN. Indeed, we were able to recapitulate the keratocyte-like phenotype on intermediate densities of BSA alone (Fig. 6a). The percentage of plated neutrophils exhibiting keratocyte-like phenotype on fields of BSA at sub-saturating density was 63 % (n = 3, SE = 22%). Furthermore, at saturating densities of BSA alone, neutrophils again switched to the amoeboid phenotype (Fig. 6b). The percentage of plated neutrophils exhibiting amoeboid phenotype on fields of BSA at saturating density was 73% (n = 1, SD = 4%). When we repeated the function-blocking antibody study on neutrophils exposed to intermediate-density BSA substrates, we again found that MAC-1 was mediating adhesion (Fig. 6c).

The finding that neutrophils were employing the promiscuous integrin MAC-1 to mediate adhesion to our experimental surfaces reinforces the necessity of choosing an appropriate blocking reagent against non-specific cell adhesion. BSA, which is often used to block surfaces, actually functions as an adhesive ligand. Coating surfaces with Pluronic is the only method we have found to reliably eliminate all non-specific background adhesion in our *in vitro* motility assays. This type of exquisite discrimination of the roles of different ligands is only possible with improved surface techniques, such as microcontact printing.[9]

Aside from the obvious conclusion that care must be taken to block non-specific binding with appropriately neutral ligands, future work will address how the organization and density of adhesion ligands leads to the morphology of cell response. Now, we can speculate that a high density of adhesion ligands over a large spatial domain promotes uropod formation. If this is the case, distribution of ligands into patches would prevent uropod formation, even if the density in the patches were locally high.

## Conclusions

Our work has demonstrated that neutrophils are capable of a phenotypic switch in morphology and associated motility as dictated by adhesion ligand density. The nature of the density sensing remains to be addressed in determining whether neutrophils are sensitive to these changes at the receptor length scale or across their total cell-substrate contact area. We anticipate microcontact printing will be a useful platform in addressing this question. By quantifying the motility associated with the amoeboid and keratocyte-like phenotypes we found the modes of migration to be distinct. The biophysical mechanism that underpins these differences is unclear. We suspect visualizing cytoskeletal architectures will improve our mechanistic insight. Lastly, our finding that the integrin heterodimer MAC-1 was being employed to mediate adhesion to our experimental surfaces reinforces the importance of avoiding BSA as an agent to block non-specific binding in neutrophils.

## Supplementary Material

Refer to Web version on PubMed Central for supplementary material.

## Acknowledgements

We are grateful to Eric Johnston for technical assistance in the laboratory and Professor Chistopher S. Chen, Michael T. Yang, PhD and Ravi A. Desai, PhD for their time and expertise in teaching us microcontact printing. Funding for this work was provided by a National Science Foundation Graduate Research Fellowship to SJH and a grant from the National Institutes of Health (HL18208) to DAH.

## References

1. Nathan C. Neutrophils and immunity: challenges and opportunities. Nat Rev Immunol. 2006; 6:173–182. DOI: 10.1038/nri1785. [PubMed: 16498448]
2. McDonald B, Pittman K, Menezes GB, Hirota SA, Slaba I, Waterhouse CCM, Beck PL, Muruve DA, Kubes P. Intravascular Danger Signals Guide Neutrophils to Sites of Sterile Inflammation. Science. 2010; 330:362–366. DOI: 10.1126/science.1195491. [PubMed: 20947763]
3. (a) Irimia D, Liu S-Y, Tharp WG, Samadani A, Toner M, Poznansky MC. Microfluidic system for measuring neutrophil migratory responses to fast switches of chemical gradients. Lab Chip. 2006; 6:191–198. DOI: 10.1039/b511877h. [PubMed: 16450027] (b) Sackmann EK, Berthier E, Young EWK, Shelef MA, Wernimont SA, Huttenlocher A, Beebe DJ. Microfluidic kit-on-a-lid: a versatile platform for neutrophil chemotaxis assays. Blood. 2012 DOI: 10.1182/blood-2012-03-416453.
4. (a) Lammermann T, Bader BL, Monkley SJ, Worbs T, Wedlich-Soldner R, Hirsch K, Keller M, Forster R, Critchley DR, Fassler R, Sixt M. Rapid leukocyte migration by integrin-independent flowing and squeezing. Nature. 2008; 453:51–55. DOI: 10.1038/nature06887. [PubMed: 18451854] (b) Hawkins RJ, Piel M, Faure-Andre G, Lennon-Dumenil AM, Joanny JF, Prost J, Voituriez R. Pushing off the Walls: A Mechanism of Cell Motility in Confinement. Physical Review Letters. 2009; 102:058103. DOI: 10.1103/PhysRevLett.102.058103. [PubMed: 19257561] (c)

Konstantopoulos K, Wu P-H, Wirtz D. Dimensional Control of Cancer Cell Migration. Biophys J. 2013; 104:279–280. DOI: 10.1016/j.bpj.2012.12.016. [PubMed: 23442847]

5. (a) Zigmond SH. Chemotaxis by polymorphonuclear leukocytes. J Cell Biol. 1978; 77:269–87. [PubMed: 649652] (b) Malawista SE, Chevance A. d. B. Random locomotion and chemotaxis of human blood polymorphonuclear leukocytes (PMN) in the presence of EDTA: PMN in close quarters require neither leukocyte integrins nor external divalent cations. Proceedings of the National Academy of Sciences. 1997; 94:11577–11582.(c) Butler LM, Khan S, Ed Rainger G, Nash GB. Effects of endothelial basement membrane on neutrophil adhesion and migration. Cell Immunol. 2008; 251:56–61. DOI: 10.1016/j.cellimm.2008.04.004. [PubMed: 18479679] (d) Houk AR, Jilkine A, Mejean CO, Boltyanskiy R, Dufresne ER, Angenent SB, Altschuler SJ, Wu LF, Weiner OD. Membrane Tension Maintains Cell Polarity by Confining Signals to the Leading Edge during Neutrophil Migration. Cell. 2012; 148:175–188. DOI: 10.1016/j.cell.2011.10.050. [PubMed: 22265410] (e) Yanai M, Butler JP, Suzuki T, Sasaki H, Higuchi H. Regional rheological differences in locomoting neutrophils. American Journal of Physiology - Cell Physiology. 2004; 287:C603–C611. DOI: 10.1152/ajpcell.00347.2003. [PubMed: 15163623]
6. (a) Cassimeris L, McNeill H, Zigmond SH. Chemoattractant-stimulated polymorphonuclear leukocytes contain two populations of actin filaments that differ in their spatial distributions and relative stabilities. The Journal of Cell Biology. 1990; 110:1067–1075. DOI: 10.1083/jcb.110.4.1067. [PubMed: 2324192] (b) Matzner Y, Vlodavsky I, Michaeli RI, Eldor A. Selective inhibition of neutrophil activation by the subendothelial extracellular matrix: possible role in protection of the vessel wall during diapedesis. Exp Cell Res. 1990; 189:233–40. [PubMed: 2164483]
7. (a) Oakes PW, Patel DC, Morin NA, Zitterbart DP, Fabry B, Reichner JS, Tang JX. Neutrophil morphology and migration are affected by substrate elasticity. Blood. 2009; 114:1387–95. DOI: 10.1182/blood-2008-11-191445. [PubMed: 19491394] (b) Stroka KM, Aranda-Espinoza H. Neutrophils display biphasic relationship between migration and substrate stiffness. Cell Motil Cytoskeleton. 2009; 66:328–41. DOI: 10.1002/cm.20363. [PubMed: 19373775] (c) Jannat RA, Robbins GP, Ricart BG, Dembo M, Hammer DA. Neutrophil adhesion and chemotaxis depend on substrate mechanics. J Phys-Condens Mat. 2010; 22 DOI: 10.1088/0953-8984/22/19/194117.
8. (a) Barnhart EL, Lee KC, Keren K, Mogilner A, Theriot JA. An adhesion-dependent switch between mechanisms that determine motile cell shape. PLoS Biol. 2011; 9:e1001059. DOI: 10.1371/journal.pbio.1001059. [PubMed: 21559321] (b) Ziebert F, Aranson IS. Effects of adhesion dynamics and substrate compliance on the shape and motility of crawling cells. PLoS One. 2013; 8:e64511. DOI: 10.1371/journal.pone.0064511. [PubMed: 23741334]
9. Desai RA, Khan MK, Gopal SB, Chen CS. Subcellular spatial segregation of integrin subtypes by patterned multicomponent surfaces. Integr Biol (Camb). 2011; 3:560–7. DOI: 10.1039/c0ib00129e. [PubMed: 21298148]
10. Tan JL, Liu W, Nelson CM, Raghavan S, Chen CS. Simple approach to micropattern cells on common culture substrates by tuning substrate wettability. Tissue Eng. 2004; 10:865–72. DOI: 10.1089/1076327041348365. [PubMed: 15265304]
11. Crocker JC, Hoffman BD. Multiple-particle tracking and two-point microrheology in cells. Method Cell Biol. 2007; 83:141–178. DOI: 10.1016/S0091-679x(07)83007-X.
12. Chen CS, Mrksich M, Huang S, Whitesides GM, Ingber DE. Geometric control of cell life and death. Science. 1997; 276:1425–1428. DOI: 10.1126/science.276.5317.1425. [PubMed: 9162012]
13. Tan JL, Tien J, Pirone DM, Gray DS, Bhadriraju K, Chen CS. Cells lying on a bed of microneedles: An approach to isolate mechanical force. Proceedings of the National Academy of Sciences of the United States of America. 2003; 100:1484–1489. DOI: 10.1073/pnas.0235407100. [PubMed: 12552122]
14. (a) Thery M, Racine V, Pepin A, Piel M, Chen Y, Sibarita J-B, Bornens M. The extracellular matrix guides the orientation of the cell division axis. Nature Cell Biology. 2005; 7:947–953. DOI: 10.1038/ncb1307. [PubMed: 16179950] (b) Tee SY, Fu J, Chen CS, Janmey PA. Cell shape and substrate rigidity both regulate cell stiffness. Biophys J. 2011; 100:L25–7. DOI: 10.1016/j.bpj.2010.12.3744. [PubMed: 21354386] (c) Ruiz SA, Chen CS. Microcontact printing: A tool to pattern. Soft Matter. 2007; 3:168–177. DOI: 10.1039/b613349e.

15. (a) Lee D, King MR. Microcontact printing of P-selectin increases the rate of neutrophil recruitment under shear flow. Biotechnol Prog. 2008; 24:1052–9. DOI: 10.1002/btpr.35. [PubMed: 19194913] (b) Ricart BG, Yang MT, Hunter CA, Chen CS, Hammer DA. Measuring traction forces of motile dendritic cells on micropost arrays. Biophys J. 2011; 101:2620–8. DOI: 10.1016/j.bpj.2011.09.022. [PubMed: 22261049] (c) Shen K, Thomas VK, Dustin ML, Kam LC. Micropatterning of costimulatory ligands enhances CD4+ T cell function. Proceedings of the National Academy of Sciences. 2008; 105:7791–7796. DOI: 10.1073/pnas.0710295105. (d) Tong Z, Cheung LS, Stebe KJ, Konstantopoulos K. Selectin-mediated adhesion in shear flow using micropatterned substrates: multiple-bond interactions govern the critical length for cell binding. Integr Biol (Camb). 2012; 4:847–56. DOI: 10.1039/c2ib20036h. [PubMed: 22627390]

16. (a) Brown XQ, Ookawa K, Wong JY. Evaluation of polydimethylsiloxane scaffolds with physiologically-relevant elastic moduli: interplay of substrate mechanics and surface chemistry effects on vascular smooth muscle cell response. Biomaterials. 2005; 26:3123–3129. DOI: 10.1016/j.biomaterials.2004.08.009. [PubMed: 15603807] (b) Fuard D, Tzvetkova-Chevolleau T, Decossas S, Tracqui P, Schiavone P. Optimization of poly-di-methyl-siloxane (PDMS) substrates for studying cellular adhesion and motility. Microelectronic Engineering. 2008; 85:1289–1293. DOI: 10.1016/j.mee.2008.02.004.

17. Hung W-C, Chen S-H, Paul CD, Stroka KM, Lo Y-C, Yang JT, Konstantopoulos K. Distinct signaling mechanisms regulate migration in unconfined versus confined spaces. The Journal of Cell Biology. 2013; 202:807–824. DOI: 10.1083/jcb.201302132. [PubMed: 23979717]

18. (a) Dunn GA. Characterising a kinesis response: time averaged measures of cell speed and directional persistence. Agents and Actions Supplements. 1983; 12:14–33. [PubMed: 6573115] (b) Lauffenburger, DA., Linderman, JJ. Receptors: models for binding, trafficking, and signaling. Oxford University Press; New York: 1993. p. x-365.

19. Kishimoto TK, Jutila MA, Berg EL, Butcher EC. Neutrophil Mac-1 and MEL-14 adhesion proteins inversely regulated by chemotactic factors. Science. 1989; 245:1238–41. DOI: 10.1126/science.2551036. [PubMed: 2551036]

20. Schiffmann E, Corcoran BA, Wahl SM. N-formylmethionyl peptides as chemoattractants for leucocytes. Proceedings of the National Academy of Sciences. 1975; 72:1059–1062.

21. (a) van den Berg JM, Mul FP, Schippers E, Weening JJ, Roos D, Kuijpers TW. Beta1 integrin activation on human neutrophils promotes beta2 integrin-mediated adhesion to fibronectin. Eur J Immunol. 2001; 31:276–84. DOI: 10.1002/1521-4141(200101)31:1<276::AID-IMMU276>3.0.CO;2-D. [PubMed: 11265644] (b) Penberthy TW, Jiang Y, Luscinskas FW, Graves DT. MCP-1-stimulated monocytes preferentially utilize beta 2-integrins to migrate on laminin and fibronectin. Am J Physiol. 1995; 269:C60–8. [PubMed: 7543245]

22. Lishko VK, Yakubenko VP, Ugarova TP. The interplay between integrins alphaMbeta2 and alpha5beta1 during cell migration to fibronectin. Exp Cell Res. 2003; 283:116–26. DOI: 10.1016/S0014-4827(02)00024-1. [PubMed: 12565824]

23. (a) Henderson RB, Lim LH, Tessier PA, Gavins FN, Mathies M, Perretti M, Hogg N. The use of lymphocyte function-associated antigen (LFA)-1-deficient mice to determine the role of LFA-1, Mac-1, and alpha4 integrin in the inflammatory response of neutrophils. J Exp Med. 2001; 194:219–26. DOI: 10.1084/jem.194.2.219. [PubMed: 11457896] (b) Phillipson M, Heit B, Colarusso P, Liu L, Ballantyne CM, Kubes P. Intraluminal crawling of neutrophils to emigration sites: a molecularly distinct process from adhesion in the recruitment cascade. J Exp Med. 2006; 203:2569–75. DOI: 10.1084/jem.20060925. [PubMed: 17116736]

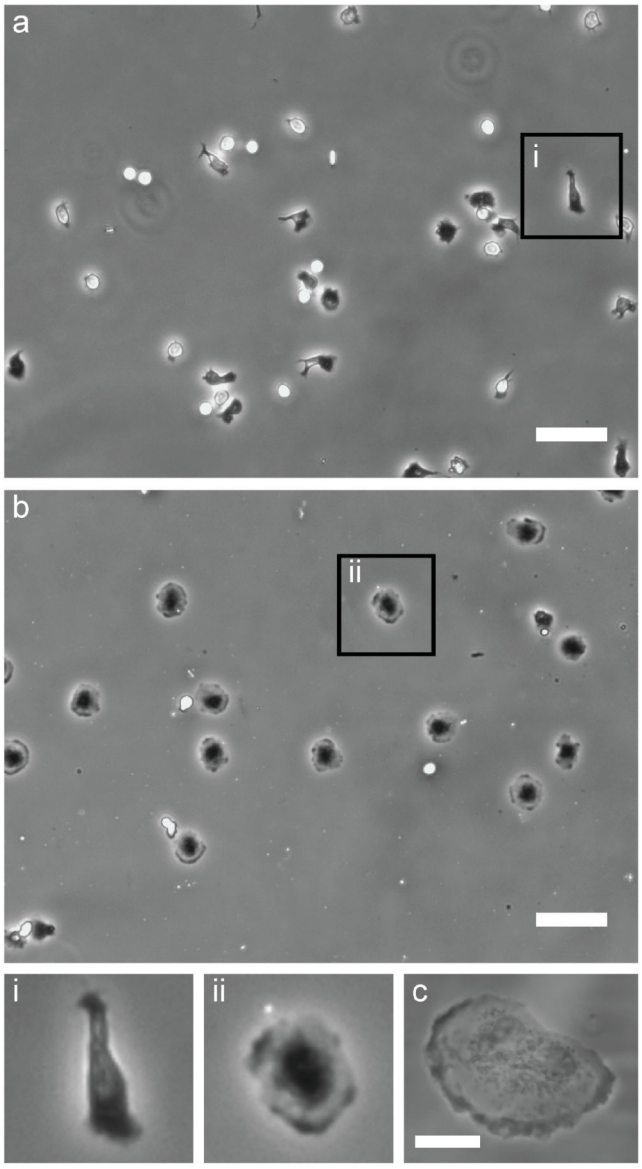


**Fig. 1. Two neutrophil morphologies**

(a) FN-adsorbed glass, blocked with BSA. Scalebar is 50 μm. Region (i) is enlarged 3×. (b) FN-printed PDMS, blocked with Pluronic. Scalebar is 50 μm. Region (ii) is enlarged 3×. (c) Same preparation as (b) but higher magnification image. Scalebar is 10 μm.

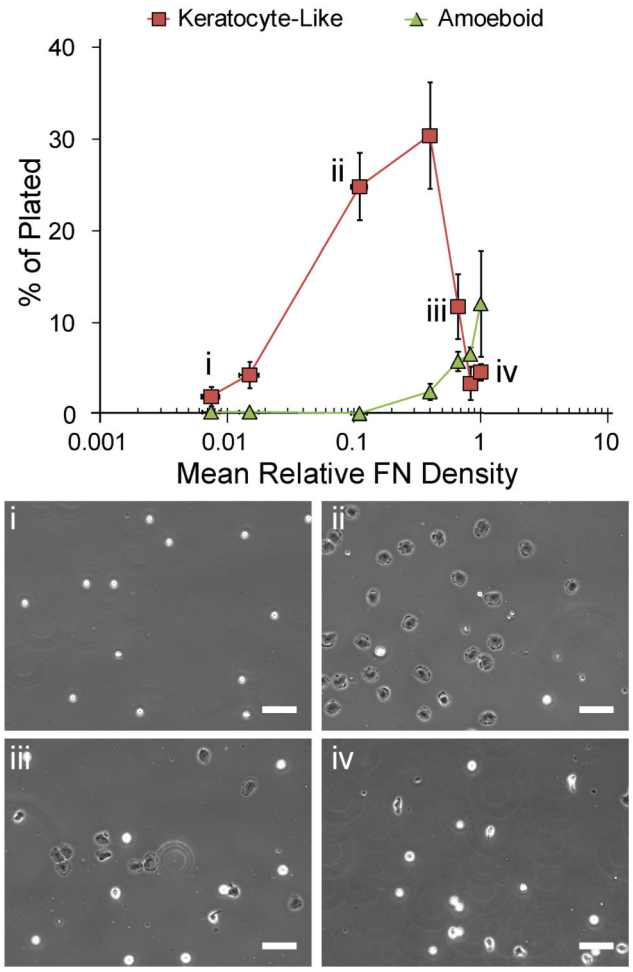


**Fig. 2. Neutrophil phenotype on increasing densities of FN**

Adherent neutrophils as percentage of total plated cells per sub-saturating densities of FN. Representative images from a single experiment on (i) 0.7% (ii) 11% (iii) 66% and (iv) 100% saturated FN substrates. Scalebars are 50 μm. Error bars are ± standard error of the mean. Substrate density was measured via quantitative fluorescence microscopy (Supplementary Fig. 4b). All substrates were FN-printed and Pluronic-blocked PDMS.

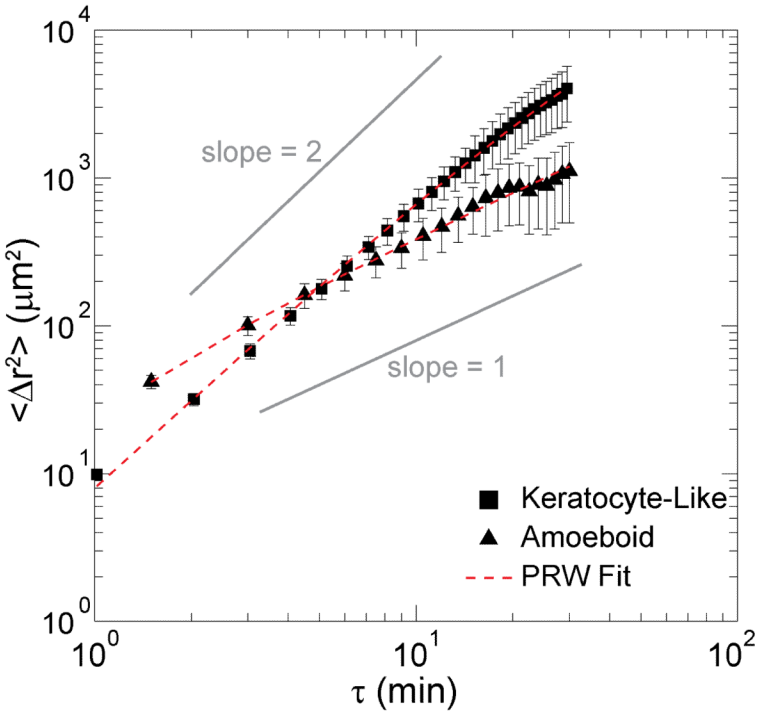


**Fig. 3. Mean squared displacements (MSDs) of two motility modes**

Time and ensemble averaged MSDs of neutrophils undergoing amoeboid motility or keratocyte-like motility. Amoeboid cells acquire displacement diffusively, slope ~ 1. Keratocyte-like cells acquire displacement superdiffusively, slope > 1. Dotted line is fit of empirical data with persistent random walk (PRW) model of cell motility. Error bars are ± standard error of the mean.

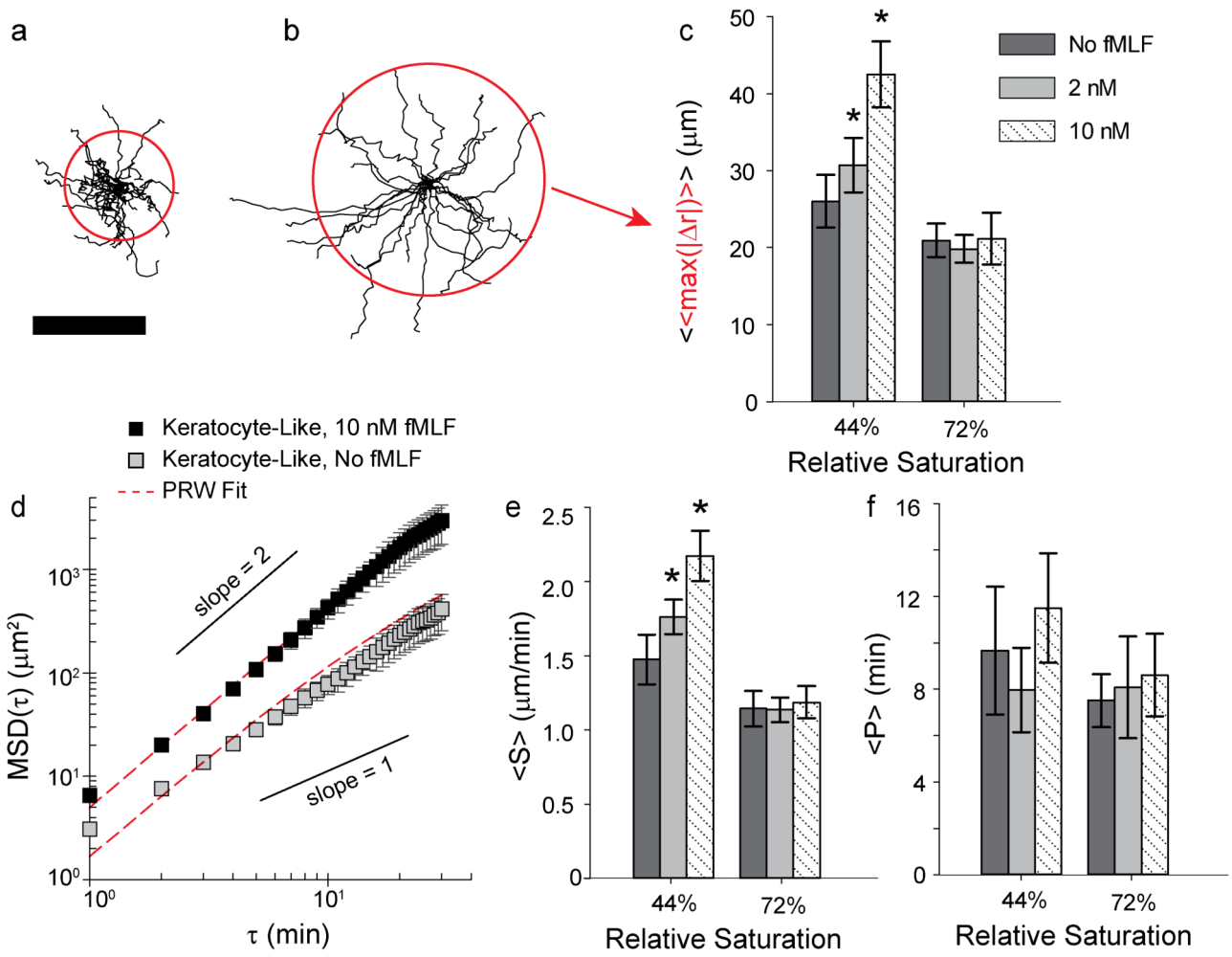


**Fig. 4. Quantification of neutrophil haptokinesis and chemokinesis of keratocyte-like phenotype**

Human neutrophil trajectories through 30 min of motility on 44% FN-saturated surface in (a) the absence of fMLF and (b) the presence of 10 nM fMLF. Scalebar is 50 μm. Solid red circle is the mean maximum displacement (<max(|Δr|)>) of 30 min neutrophil trajectories for (a) <max(|Δr|)> ~ 24 μm and (b) <max(|Δr|)> ~ 51 μm. (c) Mean of the set of mean maximum displacements for all independent observations of a particular FN density and fMLF combination tested (<<max(|Δr|)>>). (d) MSD(τ) corresponding to a single donor's neutrophils migrating on 44% FN-saturated surface in the presence or absence of fMLF. Dotted red line is fit of persistent random walk model (PRW) to empirical data. Model fit parameters (e) speed and (f) persistence. Error bars are ± standard error of the mean. Asterisk denotes significant difference relative to No fMLF condition as computed by post-hoc SNK Multiple Comparisons Method ($p < 0.05$).

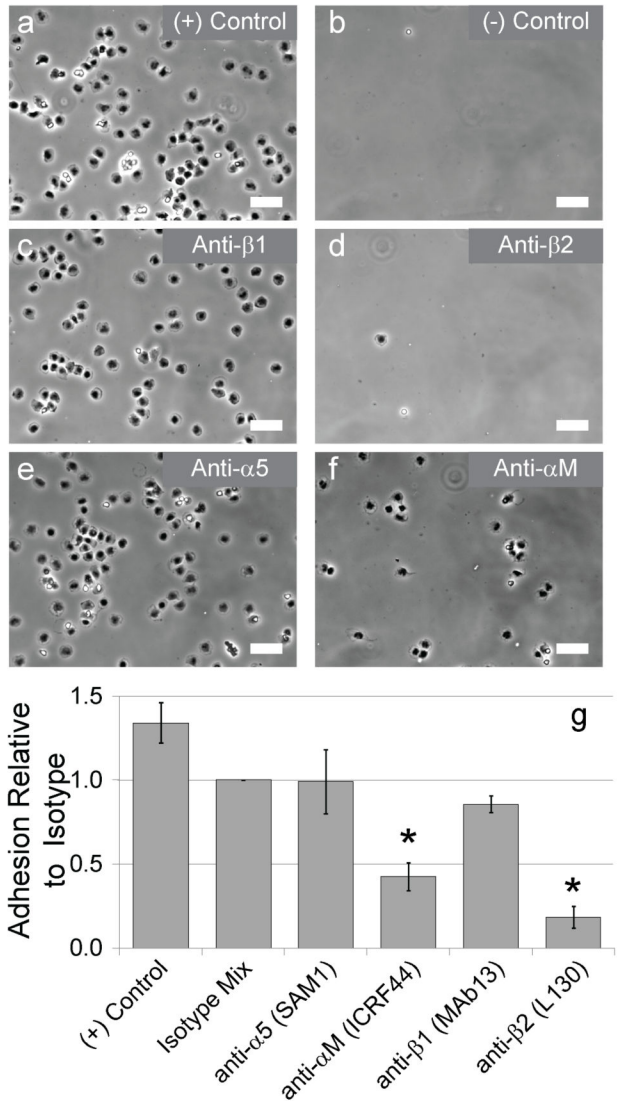


**Fig. 5. Integrin blocking on FN**

Integrin blocking of neutrophils pre-incubated with antibodies against various integrin chains before exposure to 44% FN-saturated surfrace. (a) Positive binding control, no antibodies. (b) Negative binding control, no FN, just Pluronic blocking. (c) anti-$\beta_1$ clone MAb13, (d) anti-$\beta_2$clone L130, (e) anti-$\alpha_5$ clone SAM1, and (f) anti-$\alpha_M$ clone ICRF44. Scalebars are 50 μm. (g) Mean ratio of adherent cells to isotype control. Error bars are ± standard error of the mean (n = 3-4). Asterisk denotes significant difference relative to isotype control as computed by post-hoc Dunnet's Method ($p < 0.05$).

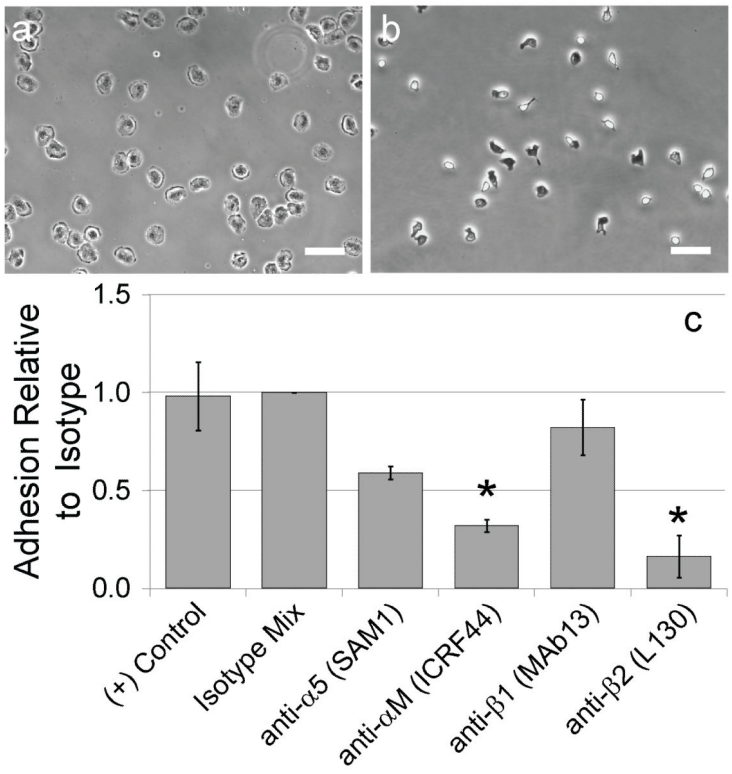


**Fig. 6. Neutrophil adhesion to BSA**

(a) Keratocyte-like phenotype of neutrophils on intermediate density of BSA. (b) Amoeboid phenotype returns on saturating density of BSA. (c) Recapitulation of antibody blocking study of neutrophils on intermediate density BSA surfaces. Mean ratio of adherent cells to isotype control. Error bars are ± standard error of the mean (n = 2-3). Asterisk denotes significant difference relative to isotype control as computed by post-hoc Dunnet's Method ($p < 0.05$.